Schiff moments of deformed nuclei

O. P. Sushkov
School of Physics, The University of New South Wales, Sydney, New South Wales 2052, Australia

(Received 15 July 2023; accepted 13 June 2024; published 8 July 2024)

Stimulated by the recent suggestion of using a europium compound for the Cosmic Axion Spin Precession Experiment search for axionlike dark matter, I develop a new method for accurate calculation of Schiff moments of even-odd deformed nuclei. The method is based on experimental data on magnetic moments and $E1$ and $E3$ transition amplitudes in the given even-odd nucleus and in adjacent even-even nuclei. Despite the fact that such data sets are not yet available for a lot of the interesting nuclei, the full set of data is available for ^{153}Eu. Hence, I perform the calculation for ^{153}Eu and find the value of the Schiff moment. The value is about 30 times larger than a typical Schiff moment of a spherical heavy nucleus. The enhancement of the Schiff moment in ^{153}Eu is related to the low-energy octupole mode. On the other hand the value of the Schiff moment I find is 30 times smaller than that obtained under the assumption of a static octupole deformation.

DOI: 10.1103/PhysRevC.110.015501

I. INTRODUCTION

The electric dipole moment (EDM) of an isolated quantum object in a nondegenerate quantum state is a manifestation of violation of time reversal (T) and parity (P) fundamental symmetries. The search for the EDM of a neutron is a long quest for fundamental P and T violation [1–3]. The EDM of a nucleus can be significantly larger than that of a neutron [4]. However a nucleus has nonzero electric charge and therefore in a charge neutral system (atom, molecule, solid) the EDM of the nucleus cannot be measured [5]. The quantity that can be measured is the so called Schiff moment (SM) which is nonzero due to the finite nuclear size [4]. Like the EDM, the SM is a vector directed along the angular momentum.

The Cosmic Axion Spin Precession Experiment (CASPEr) searches for QCD axion dark matter via an induced oscillating nuclear SM. The first-generation CASPEr experiment is based on the lead titanate ferroelectric [6] (see also Ref. [7]). The experiment is probing the oscillating SM of the ^{207}Pb nucleus. There is a recent suggestion [8] to use for the CASPEr experiment the crystal $EuCl_3 \cdot 6H_2O$ instead of lead titanate. The major advantage is experimental: a possibility to polarize Eu nuclei via optical pumping in this crystal may allow an order-of-magnitude sensitivity improvement. The expected effect in $EuCl_3 \cdot 6H_2O$ has been calculated in Ref. [9]. The observable effect in a solid has four different spatial and energy scales inside each other: (i) quark-gluon scale, $r < 1$ fm; (ii) nuclear scale, $1 \lesssim r \lesssim 10$ fm; (iii) atomic scale, $10\ \text{fm} < r \lesssim 1$ Å; and (iv) solid state scale, $r > 1$ Å. The calculation [9] is pretty accurate at the scale (iii), and it has an uncertainty at most by factor 2 at the scales (i) and (iv). However, the uncertainty at the scale (ii), the nuclear scale, is two orders of magnitude, which is the uncertainty in the ^{153}Eu Schiff moment. Such an uncertainty is typical for deformed even-odd nuclei. The aim of the present paper is twofold: (i) develop an accurate method of calculating the SM and (ii) perform the calculation of the SM of ^{153}Eu. A reliable purely theoretical calculation is hardly possible. Therefore, our approach is to use the available experimental data as much as possible.

^{153}Eu has a deformed nucleus. A simple estimate of the SM of a nucleus with a quadrupole deformation was performed in Ref. [4], with the Nilsson model as the basis. The result was an order of magnitude larger than SM of a spherical heavy nucleus, say SM of ^{207}Pb. Reference [10] then pointed out that if the nucleus has a static octupole deformation, the SM is dramatically enhanced. Based on analysis of rotational spectra of ^{153}Eu the authors of Ref. [11] argued that ^{153}Eu has a static octupole deformation and, hence, using the idea [10] arrived at the estimate of SM that is 10^3 times larger than that of a heavy spherical nucleus.

In the present paper I analyze the available experimental data on magnetic moments and amplitudes of $E1$ and $E3$ nuclear transitions of ^{153}Eu, in order to elucidate the structure of the nuclear wave function. As a result of this analysis, one can confidently claim that the model of static octupole deformation is incorrect. The Nilsson wave functions of the quadrupole deformed nucleus are good approximations. However, this does not imply that the octupole mode is irrelevant. There is an admixture of the octupole vibration to the Nilsson states and I determine the amplitude of the admixture. All in all, this allows one to perform a reliable and accurate calculation of the SM.

The effect of the dynamic octupole vibration on SM has been considered previously in Refs. [12,13]. The results of the present paper disagree with some conclusions and numerical estimates in these papers. The main difference, however, is that Refs. [12,13] are aimed at scenario building and rough general estimates. On the other hand, the present paper performs an accurate SM calculation for the specific nucleus, ^{153}Eu.

Let us emphasize that the present calculation of SM is based on the analysis of a broad set of data, therefore the statement is nucleus specific—it is valid for ^{153}Eu and it is

valid for ^{237}Np. Unfortunately such broad data sets are not yet available for many other interesting nuclei.

The structure of the paper is as follows. In Sec. II the lifetimes of the relevant levels in ^{152}Sm and ^{153}Eu are analyzed and hence the relevant $E1$ amplitudes are determined. Section III is the central one, where I discuss the structure of wave functions of the parity doublet $|5/2^{\pm}\rangle$ in ^{153}Eu. Section IV determines the quadrupole deformation of ^{153}Eu. Section V explains the parametrization used for the octupole deformation. Section VI describes the structure of octupole excitations. Section VII extracts the value of octupole deformation from experimental data. In Sec. VIII I calculate the T- and P-odd mixing of $5/2^+$ and $5/2^-$ states in ^{153}Eu. The EDM of the ^{153}Eu nucleus is calculated in Sec. IX, and the SM of the ^{153}Eu nucleus is calculated in Sec. X. Section XI presents the conclusions of the paper.

II. EXPERIMENTAL $E1$ AMPLITUDES IN ^{152}Sm AND ^{153}Eu

All data used in this section are taken from Ref. [14]. Even-even nuclei in the vicinity of ^{153}Eu have a low-energy ≈1-MeV collective octupole excitation. There is the quadrupole ground-state rotational band and the octupole rotational band starting at the energy of the octupole excitation. As a reference even-even nucleus I take ^{152}Sm. In principle ^{154}Sm could also do the job, but the data for ^{154}Sm are much less detailed, especially electron scattering data that are discussed in Sec. VII. The energies of the relevant states of the octupole band in ^{152}Sm are $E(1^-) = 963$ keV and $E(3^-) = 1041$ keV. The half-life of the 1^- state is $t_{1/2} = 28.2$ fs, hence the lifetime is $\tau(1^-) = 28.2/\ln(2) = 40.7$ fs. The state decays via the $E1$ transition to the ground state, 0^+, and to the 2^+ state of the ground-state rotational band. The decay branching ratio is $W(0^+)/W(2^+) = 0.823$. Therefore, the partial lifetime for the $1^- \to 0^+$ transition is $\tau_{\rm partial} = 90$ fs. The $1^- \to 0^+$ $E1$ transition decay rate is given by [15]

$$\frac{1}{\tau_{\rm partial}} = \frac{4\omega^3}{3(2j+1)}|\langle j'||d||j\rangle|^2, \tag{1}$$

where ω is the γ-quantum frequency and d is the electric dipole operator. The reduced matrix element of the dipole moment can be expressed in terms of d_z in the proper reference frame of the deformed nucleus [16]:

$$|\langle j'||d||j\rangle|^2 = \left|\sqrt{(2j+1)(2j'+1)}\begin{pmatrix} j' & 1 & j \\ -m & 0 & m\end{pmatrix}\right|^2 \times |\langle 0|d_z|1\rangle|^2. \tag{2}$$

For the $1^- \to 0^+$ transition $j = 1$, $j' = 0$, and $m = 0$. Hence

$$\langle 0|d_z|1\rangle = +e \times 0.31 \text{ fm}. \tag{3}$$

Here $e = |e|$ is the elementary charge.

^{153}Eu is a deformed nucleus with the ground state $|5/2^+\rangle$. The nearest opposite parity state $|5/2^-\rangle$ has energy $E = 97.4$ keV. The half-life of the $|5/2^-\rangle$ state is $t_{1/2} = 0.20$ ns, hence the lifetime is $\tau(5/2^-) = 0.29$ ns. The lifetime is due to the $E1$ decay $|5/2^-\rangle \to |5/2^+\rangle$. Using Eqs. (1) and (2) with $j = j' = m = 5/2$ and comparing with experiments one finds the corresponding d_z in the proper reference frame:

$$\langle 5/2^+|d_z|5/2^-\rangle = -e \times 0.12 \text{ fm}. \tag{4}$$

Of course lifetimes cannot be used to determine signs in Eqs. (3) and (4). Section VI explains how these signs are determined.

III. THE WAVE FUNCTIONS OF THE GROUND-STATE PARITY DOUBLET $|\frac{5}{2}^{\pm}\rangle$ IN ^{153}Eu

The standard theoretical description of low-energy states in ^{153}Eu is based on the Nilsson model of a quadrupole-deformed nucleus. In agreement with experimental data, the Nilsson model predicts the spin and parity of the ground state, $5/2^+$. It also predicts the existence of the low-energy excited state with opposite parity, $5/2^-$. The wave functions of the odd proton in the Nilsson scheme are $|5/2^+\rangle = |413\frac{5}{2}\rangle$ and $|5/2^-\rangle = |532\frac{5}{2}\rangle$. The explicit form of these wave functions is presented in the Appendix. There are two rotational towers built on these states.

An alternative to the Nilsson approach is the model of a static collective octupole deformation [11]. In this model the odd proton moves in the pear shape potential forming the $\Omega = 5/2$ single-particle state. A rotational tower built on this odd proton state is consistent with the observed spectra, and this is why the paper [11] argues in favor of the static octupole deformation. However, two different parity rotational towers in the Nilsson scheme are equally consistent with observed spectra. Therefore, based solely on nuclear spectra, one can conclude only that both the Nilsson model and the static octupole deformation model are consistent with the data. Additional data are needed to distinguish between these two models.

The Nilsson model explains the $5/2$ ground-state angular momentum, while in the static octupole model this value appears from nowhere. However, in principle it is possible that accidentally the single-particle state in the pear shape potential has $\Omega = 5/2$.

To distinguish between the two models, let us examine magnetic moments. The measured magnetic moment of the ground state is $\mu_{5/2^+} = 1.53\mu_N$ (see Ref. [14]). This value is consistent with prediction on the Nilsson model [17]. The magnetic moment of the $5/2^-$ state has some ambiguity: the measurement led to two possible interpretations, "the recommended value" $\mu_{5/2^-} = 3.22\mu_N$ and another value consistent with measurement $\mu_{5/2^-} = -0.52\mu_N$ (see Ref. [14]). The recommended value is consistent with the prediction of the Nilsson model [18]. Thus the magnetic moments are consistent with the Nilsson model. The static octupole model predicts $\mu_{5/2^-} \approx \mu_{5/2^+}$, which is inconsistent with experimental data.

While the arguments presented above rule out the static octupole model, they do not imply that the octupole mode is irrelevant; actually it is relevant. I will show now that, while the Nilsson model explains the magnetic moments, it cannot explain the $E1$ transition amplitudes.

Within the Nilsson model one can calculate the $E1$ dipole transition matrix element $\langle 5/2^+|d_z|5/2^-\rangle$. A straightforward calculation with wave functions (A4) gives the dipole matrix

element

$$d_z = e(1-Z/A)\left\langle 532\frac{5}{2}\middle|z\middle|413\frac{5}{2}\right\rangle$$
$$= e(1-Z/A)\frac{z_0}{\sqrt{2}}(0.527-0.510+0.017)$$
$$= e\times 0.036\ \text{fm}. \tag{5}$$

Here the effective proton charge $(1-Z/A)=0.59$ has been accounted for. The calculated matrix element (5) is three times smaller than the experimental one (4). The first impression is that the disagreement is not bad, having in mind the dramatic compensations in Eq. (5). However, there are the following two observations.

(i) It has been pointed out in Ref. [4] that the compensation in (5) is not accidental: the compensation is due to the structure of Nilsson states, and the matrix element $\langle 532\frac{5}{2}|z|413\frac{5}{2}\rangle$ is proportional to the energy splitting $E_{5/2^-}-E_{5/2^+}$. The matrix element is small because the splitting is small, compared to the shell model energy $\omega_0\approx 7.7$ MeV. The value (5) is calculated with wave functions from Ref. [19] that correspond to $E_{5/2^-}-E_{5/2^+}\approx 450$ keV. On the other hand, for ^{153}Eu $E_{5/2^-}-E_{5/2^+}\approx 97$ keV. Therefore, the true matrix element must be even smaller than the value (5).

(ii) The electric dipole operator is T even. Therefore, there is a suppression of the matrix element due to pairing of protons, $d_z\to d_z(u_1u_2-v_1v_2)$, where u and v are pairing BCS factors. This further reduces the matrix element (see Ref. [20]).

The arguments in the previous paragraph lead to the conclusion that, while the Nilsson model correctly predicts the quantum numbers and explains the magnetic moments, the model does not explain the electric dipole transition amplitude. The experimental amplitude is an order of magnitude larger than the Nilsson one. This observation has been made already in Ref. [4] and confirmed in Ref. [21].

An admixture of the collective octupole to Nilsson states resolves the dipole moment issue. The first time this explanation was suggested was probably in Ref. [21]. Let us expand the ^{153}Eu nuclear wave functions

$$|+\rangle=\left|\frac{5}{2}^+\right\rangle=\sqrt{1-\alpha^2}\left|413\frac{5}{2}\right\rangle|0\rangle-\alpha\left|532\frac{5}{2}\right\rangle|1\rangle,$$
$$|-\rangle=\left|\frac{5}{2}^-\right\rangle=\sqrt{1-\alpha^2}\left|532\frac{5}{2}\right\rangle|0\rangle-\alpha\left|413\frac{5}{2}\right\rangle|1\rangle, \tag{6}$$

where α is a mixing coefficient and the states $|0\rangle$ and $|1\rangle$ describe the collective octupole mode: $|0\rangle$ is the symmetric octupole vibration and $|1\rangle$ is the antisymmetric octupole vibration. The state $|0\rangle$ corresponds to the ground state of ^{152}Sm and $|1\rangle$ corresponds to the octupole excitation at energy $\approx$1 MeV. Section VI discusses the specific structure of the states $|0\rangle$ and $|1\rangle$, explains why the mixing coefficient in both states in (6) is the same, and explains why $\alpha>0$.

Using (6) and neglecting the small single-particle contribution, the transition electric dipole moment is given by

$$\left\langle\frac{5}{2}^+\middle|d_z\middle|\frac{5}{2}^-\right\rangle=-2\alpha\sqrt{1-\alpha^2}\langle 0|d_z|1\rangle. \tag{7}$$

Hence, using the experimental values (3) and (4) one finds

$$\alpha\approx\frac{0.12}{2\times 0.31}=0.20. \tag{8}$$

Thus the weight of the admixture of the collective vibration to the simple Nilsson state is just $\alpha^2=4\%$. This weight is sufficiently small to make the Nilsson scheme calculation of magnetic moments correct. On the other hand, the weight is sufficiently large to influence electric dipole transition matrix elements.

Let us note that, under the approximation that proton and neutron distributions are identical, the octupole vibration does not have an electric dipole transition matrix element, due to the elimination of the zero mode. However, a small shift of the neutron distribution with respect to the proton distribution, in combination with the octupole deformation, does give rise to a nonzero value of the dipole matrix element: $\langle 1|d_z|0\rangle\neq 0$ (see, e.g., Refs. [22–24]). While this issue is important theoretically, pragmatically it is not important for the present analysis since I take both values of matrix elements (3) and (4) from experiment.

It is worth noting also that in the static octupole model one expects $\langle 5/2^+|d_z|5/2^-\rangle=\langle 0|d_z|1\rangle=+e\times 0.31$ fm, which is, like magnetic moments, inconsistent with experimental data.

IV. THE QUADRUPOLE DEFORMATION OF ^{153}Eu

The standard way to describe nuclear deformation is to use parameters β_l. In the corotating reference frame the surface of a quadrupole-deformed nucleus is given by

$$R(\theta)=R_0(1+\beta_2Y_{2,0}),$$
$$R_0=r_0A^{1/3},$$
$$r_0\approx 1.2\ \text{fm}, \tag{9}$$

where A is the number of nucleons and β_2^2 is neglected compared to 1.

Let us determine β_2 using the known electric quadrupole moment Q in the ground state of ^{153}Eu. There are two contributions in Q: (i) the collective contribution due to collective deformation and (ii) the single-particle contribution of the odd proton. Using the Nilsson wave functions it is easy to check that the single-particle contribution is about 3–4% of the experimental value of Q, so it can be neglected. The collective electric quadrupole moment is given by density of protons ρ_p:

$$Q_0=Q_{zz}=\int\rho_p(3z^2-r^2)dV=4\sqrt{\frac{\pi}{5}}\int\rho_pr^2Y_{20}dV$$
$$=\frac{3ZR_0^2}{\sqrt{5\pi}}\beta_2\left[1+\frac{2\sqrt{5}}{7\sqrt{\pi}}\beta_2+\frac{12}{7\sqrt{\pi}}\beta_4\right]. \tag{10}$$

Here I also include β_4 and Z is the nuclear charge. Equation (10) gives the quadrupole moment in the proper

reference frame. In the laboratory frame, for the ground state $J = \Omega = 5/2$, the quadrupole moment is $Q = \frac{5}{14}Q_0$ [see Sec. 119 (Deformed Nuclei) in Ref. [16]]. The experimental value of the ground-state quadrupole moment of ^{153}Eu is $Q = 2.412$ b [14]. From here, assuming $\beta_4 = 0.07$, one finds the quadrupole deformation of the ^{153}Eu nucleus in the ground state:

$$\beta_2 \approx 0.29. \tag{11}$$

The values $\beta_2 \approx 0.29$ and $\beta_4 = 0.07$ are in agreement with those in ^{152}Sm, determined from electron scattering [25].

The electric quadrupole moment of the ^{151}Eu nucleus in the ground state is $Q = 0.903$ b [14]. Therefore the quadrupole deformation of ^{151}Eu, $\beta_2 \approx 0.12$, is significantly smaller than that of ^{153}Eu.

V. THE NUCLEAR DENSITY VARIATION DUE TO THE OCTUPOLE DEFORMATION

The standard way to describe the static octupole deformation β_3 is to use the parametrization (9):

$$R(\theta) = R_0(1 + \beta_1 Y_{10} + \beta_2 Y_{2,0} + \beta_3 Y_{3,0} + \dots). \tag{12}$$

This equation describes the surface of the nucleus in the proper reference frame. The dipole harmonic Y_{10} is necessary to eliminate the zero mode, i.e., to satisfy the condition

$$\langle z \rangle = \int \rho(r) r Y_{10} dV = 0 \tag{13}$$

where $\rho(r)$ is the number density of nucleons. From Eq. (13) one finds

$$\beta_1 = -x\beta_2\beta_3, \quad x = \sqrt{\frac{243}{140\pi}} \approx 0.743. \tag{14}$$

Rather than using Eq. (12), for our purposes it is more convenient to use a slightly different parametrization:

$$\rho' = \beta_3 \frac{3A}{4\pi R_0^2} \delta[r - R_0(1 + \beta_2 Y_{20})](Y_{30} - x\beta_2 Y_{10}), \tag{15}$$

where ρ' is the octupole component of the nuclear density and δ is the δ function. Due to this δ function, ρ' is nonzero only at the surface of the nucleus. Parametrizations (12) and (15) are equivalent: they both satisfy the constraint (13) and both give the same octupole moment:

$$Q_{30} = \sqrt{\frac{4\pi}{7}} \int \rho r^3 Y_{30} dV = \beta_3 \frac{3A}{\sqrt{28\pi}} R_0^3. \tag{16}$$

VI. THE STRUCTURE OF THE VIBRATIONAL STATES |0⟩ AND |1⟩

The picture described in Secs. IV and V is purely classical, with static quadrupole and octupole deformations. In reality, while the quadrupole deformation is static the octupole one is dynamic. There are two different approaches to describe the octupole dynamics. Within the standard textbook approach [19], based on noninteracting phonons, the octupole vibration in a deformed nucleus is similar to that in a spherical nucleus. In this language the dynamic octupole phonon corresponds to the $|3^-\rangle$ excited state in the laboratory frame. An alternative approach (see, for example, Refs. [12,26]) considers the octupole deformation dynamics along the z axis, defined by the static quadrupole deformation. The pear dynamics along the z axis is described by a double well potential. Hence, there is a hidden octupole deformation in both the ground state and the "octupole excitation." The difference between the ground state $|0\rangle$ and the octupole excitation $|1\rangle$ is only in the symmetry of the wave function, as it is illustrated in Fig. 1. For physical intuition one could call the first approach the "atomiclike basis" and the second approach the "molecularlike basis." In both approaches only the off-diagonal matrix element of the octupole deformation is nonzero: $\beta_3 \propto \langle 3^-|\hat{\beta}_3|0\rangle \neq 0$. If β_3 is extracted from experiment and if the octupole excitation energy ΔE is much larger than all other energy scales in the problem both approaches give the same answer. In ^{153}Eu and ^{152}Sm the energy $\Delta E \approx 1$ MeV is large and hence any approach is applicable. However, the aim of this paper is not only to perform calculation of SM for ^{153}Eu, but to also develop a general calculation method that is valid for small ΔE. This is why in this paper the second approach is employed. It should be noted that a recent mean-field nuclear DFT calculation [27] does not indicate a double well structure in ^{152}Sm. However, in ^{152}Sm the tunneling matrix element between the wells is $\sim\Delta E \sim 1$ MeV. The validity of a mean field approach with such fast tunneling is questionable. In any case, for such a large ΔE, the final answer is independent of the approach, since the relevant matrix elements are extracted from experiment.

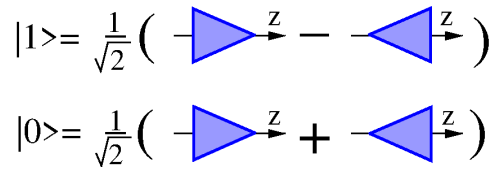

FIG. 1. A schematic representation of the states $|0\rangle$ and $|1\rangle$.

Tunneling between the two orientations of the pear leads to the energy splitting and to formation of symmetric and antisymmetric states $|0\rangle$ and $|1\rangle$, as shown in Fig. 1. In ^{152}Sm the tunneling energy splitting, $\Delta E \sim 1$ MeV, is much larger than the rotational energy splitting, $\Delta E_{\rm rot} \sim 20$ keV. Hence, there are well defined rotational towers built on $|0\rangle$ and $|1\rangle$ states (see Ref. [14]). Note that the approach I am using is valid even if the pear tunneling amplitude is comparable with the rotational energy, $\Delta E \sim \Delta E_{\rm rot}$. Of course a calculation of SM in this case is more involved because one has to diagonalize the pear tunneling and pear rotations simultaneously. Note that the case $\Delta E \sim \Delta E_{\rm rot}$ is still not the static deformation case. To have a truly static octupole one needs to have $\Delta E \ll \Delta E_{\rm rot}$.

The Hamiltonian for the odd proton reads

$$H = \frac{p^2}{2m} + U(r), \tag{17}$$

where $U(r)$ is the self-consistent potential of the even-even core. It is well known that the nuclear density $\rho(r)$ has approximately the same shape as the potential

$$U(r) \approx \frac{U_0}{\rho(0)} \rho(r), \tag{18}$$

where $U_0 \approx -50$ MeV and $\rho(0) = 3/(4\pi r_0^3)$. Hence the variation of the potential related to the octupole deformation is

$$\delta U = \frac{U_0}{\rho(0)}\rho' = \beta_3 U_0 R_0 \delta[r - R_0(1 + \beta_2 Y_{20})](Y_{30} - x\beta_2 Y_{10}). \tag{19}$$

This is the perturbation that mixes single-particle Nilsson states, with simultaneous mixing of $|0\rangle$ and $|1\rangle$. The mixing matrix element is

$$M = \langle 1|\left\langle 532\frac{5}{2}\right|\delta U\left|413\frac{5}{2}\right\rangle|0\rangle = \int \rho_{SP}(r)\delta U(r)dV,$$
$$\rho_{SP}(r) = \langle \psi^*_{532}(r)\psi_{413}(r)\rangle. \tag{20}$$

Here ρ_{SP} is the off-diagonal single-particle density of Nilsson wave functions (A4), the density depends on r, and the brackets $\langle..\rangle$ in ρ_{SP} denote averaging over spin only. Numerical evaluation of the mixing matrix element is straightforward: the answer at $\beta_2 = 0.29$ is $M \approx 5\beta_3$ MeV. The value has a slight dependence on β_2: at $\beta_2 = 0$ the value of M is 10% smaller.

In Sec. III, Eq. (6) the mixing between single-particle Nilsson states was parametrized by the coefficient α, given by

$$\alpha = \frac{M}{\Delta E}, \tag{21}$$

where $\Delta E \approx 1$ MeV. Equations (20) and (21), together with the positive value of M, explain why the coefficient α is the same in both of Eqs. (6) and why $\alpha > 0$.

Moreover, comparing Eq. (21) with the value of α extracted from experimental data [Eq. (8)], one determines the octupole deformation: $\beta_3 = 0.04$. While the value is reasonable, unfortunately there is no certainty that it is accurate. The shape approximation (18) is not very accurate. Even more importantly, it is not clear how the BCS factor influences ρ_{SP}. The BCS factor can easily reduce ρ_{SP} by factor ~2–3, hence increasing β_3 by the same factor. Theoretical calculations of β_3 give values from 0.05 [24], to 0.075 [28], and even 0.15 [29].

VII. THE VALUE OF THE OCTUPOLE DEFORMATION PARAMETER β_3

With the wave functions schematically shown in Fig. 1 one immediately finds the electric octupole matrix element between states $|0\rangle$ and $|1\rangle$:

$$\langle 1|Q^{(e)}_{30}|0\rangle = e\frac{Z}{A}Q_{30}, \tag{22}$$

where Q_{30} is given by Eq. (16). I am not aware of direct measurements of $Q^{(e)}_{30}$ in ^{152}Sm. Reference [19] presents the "oscillator strengths" for corresponding $E3$ transitions in ^{152}Sm and ^{238}U. For ^{152}Sm, $B_3 = 1.2 \times 10^5\, e^2\,\text{fm}^6$, and for ^{238}U, $B_3 = 5 \times 10^5\, e^2\,\text{fm}^6$ (Table 6.14 in Ref. [19]). However, these values have not been determined from direct electromagnetic measurements, but were instead indirectly extracted from deuteron scattering from the nuclei. For ^{238}U there is a more recent value determined from the electron scattering [30]: $B_3 = (6.4 \pm 0.6) \times 10^5\, e^2\,\text{fm}^6$. All in all, these data give $\beta_3 \approx 0.08$ for both ^{152}Sm and ^{238}U.

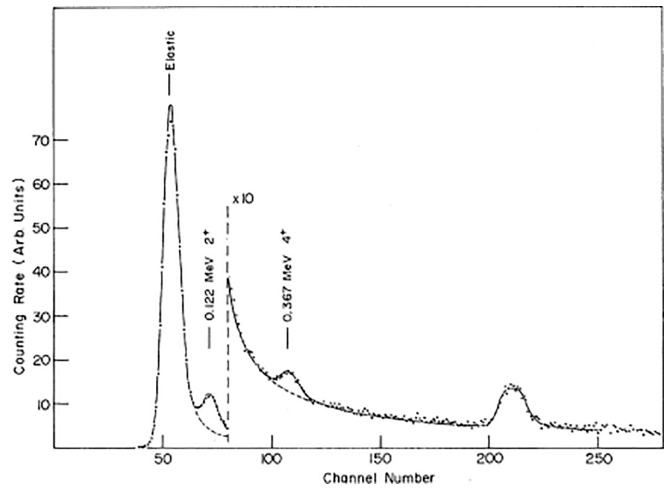

FIG. 2. The spectrum of scattered electrons from ^{152}Sm at 93.5°. Incident electron energy: 76 MeV. Aside from the ground-state rotational band, the 3^- level at 1.041 MeV and the 2^+ level at 1.086 MeV are seen (channel 210). The plot is taken from Ref. [25].

Fortunately, existing electron scattering data of Ref. [25] allow us to accurately determine β_3 in ^{152}Sm. The goal of Ref. [25] was to determine β_2 and β_4, and their results, $\beta_2 = 0.287 \pm 0.003$ and $\beta_4 = 0.070 \pm 0.003$, are remarkably close to that obtained for ^{153}Eu in Sec. IV.

Let us reanalyze the inelastic scattering spectrum of Ref. [25], a copy of which is shown in Fig. 2. The first inelastic peak at $E = 122$ keV (≈ channel 73) corresponds to the 2^+ excitation of the rotational ground-state band. The peak, after background subtraction, is shown in Fig. 3(a). Red dots are experimental points and the solid curve is the Gaussian fit:

$$I = Ae^{-(x-x_0)^2/\sigma^2},$$
$$A = 7.23,\ x_0 = 72.9,\ \sigma = 5.21. \tag{23}$$

Hence, the half width is $\Gamma = 2\ln(2)\sigma = 49.3$ keV, where I take into account that one channel step is 6.82 keV. This

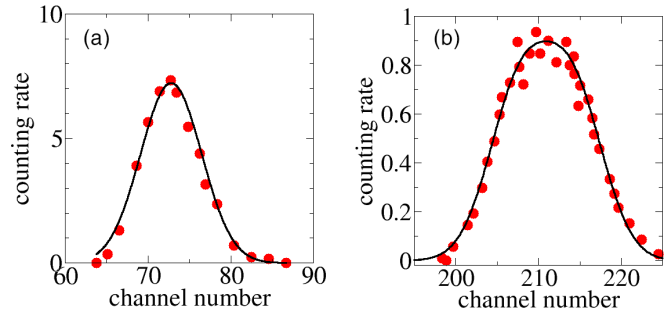

FIG. 3. Excitation peaks with subtracted background. Red dots are experimental data and black curves are Gaussian (double Gaussian) fits. (a) The 2^+ excitation of the ground-state rotational band. (b) The combined peak of the 3^- octupole and the $\gamma 2^+$ state of the rotational γ band.

energy resolution is 0.065% of the electron energy 76 MeV. This is slightly smaller than but close to the "typical value" 0.08% mentioned in Ref. [25]. The peak in Fig. 2 near channel 210 is a combination of the 3^- octupole ($E = 1041$ keV) and of the $\gamma 2^+$ state of the γ band ($E = 1086$ keV). This peak, after background subtraction, is shown in Fig. 3(b). I fit the peak by the double Gaussian:

$$I = B[e^{-(x-x_1)^2/\sigma^2} + e^{-(x-x_2)^2/\sigma^2}],$$
$$B = 0.670,\ x_1 = 207.6,\ x_2 = 214.2,\ \sigma = 5.21. \quad (24)$$

In this fit B is the only free parameter. The value of x_1 is fixed, corresponding to $E = 1041$ keV; the value of x_2 is fixed, corresponding to $E = 1086$ keV; and σ is fixed at the best-fit value in Eq. (23). The fit shows that the intensities of the 3^- and $\gamma 2^+$ lines cannot differ by more than 5%, so I set them to be equal.

Based on Eqs. (23) and (24) one finds the ratio of the spectral weights:

$$\frac{S(3^-)}{S(2^+)} = \frac{B}{A} = 0.093. \quad (25)$$

Here 2^+ is the ground-state rotational state, but, interestingly, the analysis can also give the spectral weight of the $\gamma 2^+$ state. This could allow one to determine the magnitude of the γ deformation. However, this issue is irrelevant to the Schiff moment and therefore I do not analyze it further.

The Coulomb potential of the Eu nucleus at $r \approx R_0$ is 15 MeV, which is significantly smaller than the electron energy 76 MeV. Therefore the electron wave function can be approximated as a plane wave. The momentum transfer is

$$q = 2p\sin(93.5^\circ/2) \approx 111\,\text{MeV} \approx 0.562\,\text{fm}^{-1}. \quad (26)$$

Using the expansion of the plane wave in spherical harmonics, together with the Wigner-Eckart theorem, the spectral weights can be expressed as integrals in the corotating reference frame:

$$S(2^+) \propto \left|\int Y_{20} j_2(qr)\rho(r)dV\right|^2,$$
$$S(3^-) \propto \left|\int Y_{30} j_3(qr)\rho'(r)dV\right|^2, \quad (27)$$

where $j_l(qr)$ is the spherical Bessel function [16], $\rho(r)$ is the nuclear density with quadrupole deformation, and ρ' is the octupole component of the nuclear density, given by Eq. (15). The coefficient of proportionality in both of Eqs. (27) is the same and therefore I skip it. Evaluation of integrals in (27) is straightforward; it gives

$$\int Y_{20} j_2(qr)\rho(r)dV \propto \beta_2 j_2(qR_0) = 0.302\beta_2,$$
$$\int Y_{30} j_3(qr)\rho'(r)dV \propto \beta_3 j_3(qR_0) = 0.205\beta_3. \quad (28)$$

Comparing the theoretical ratio with its experimental value (25) and using the known quadrupole deformation one finds the octupole deformations $\beta_3 = 0.45\beta_2 = 0.130$.

In the previous paragraph the plane wave approximation has been used for the electron wave function, neglecting the Coulomb potential ≈15 MeV compared to the electron energy 76 MeV. A simple way to estimate the Coulomb correction is to change $q \to q' \approx q(1 + 15/76) = 0.673\ \text{fm}^{-1}$. This results in $\beta_3 = 0.090$. This rough correction probably overestimates the effect of the Coulomb potential. An accurate calculation of the distorted electron wave functions would allow one to determine β_3 very accurately. For now I take

$$\beta_3 = 0.10. \quad (29)$$

VIII. THE T- AND P-ODD MIXING OF $5/2^+$ AND $5/2^-$ STATES IN ^{153}Eu

The operator of the T- and P-odd interaction reads [4]

$$H_{TP} = \eta\frac{G}{2\sqrt{2}m}\vec{\sigma}\cdot\vec{\nabla}\rho, \quad (30)$$

where m is the nucleon mass, $G \approx 1.03/m^2$ is the Fermi constant, η is a dimensionless constant characterizing the interaction, $\vec{\sigma}$ is the Pauli matrix corresponding to the spin of the unpaired nucleon, and ρ is the nuclear number density. The single-particle matrix element of H_{TP} between Nilsson states can be estimated as (see Ref. [4])

$$\langle 532|H_{TP}|413\rangle$$
$$\propto \langle 532|\nabla\rho|413\rangle \propto \langle 532|\nabla U|413\rangle$$
$$\propto \langle 532|[p,H]|413\rangle \propto (E_{532} - E_{413})\langle 532|p|413\rangle$$
$$\propto (E_{532} - E_{413})\langle 532|[r,H]|413\rangle$$
$$\propto (E_{532} - E_{412})^2\langle 532|r|413\rangle.$$

Thus, the matrix element is suppressed by the small parameter $[(E_{532} - E_{412})/\omega_0]^2$, with $E_{532} - E_{412} \approx 100$ keV and $\omega_0 \approx 8$ MeV. Hence the single-particle matrix element can be neglected.

The matrix element between the physical states, given in Eq. (6), also contains the collective octupole contribution:

$$\langle -|H_{TP}|+\rangle = -\alpha\left\langle 532\frac{5}{2}\middle|\langle 1|H_{TP}|0\rangle\middle|532\frac{5}{2}\right\rangle - \alpha\left\langle 413\frac{5}{2}\middle|\langle 0|H_{TP}|1\rangle\middle|413\frac{5}{2}\right\rangle. \quad (31)$$

Integrating by parts one transforms this to

$$\langle -|H_{TP}|+\rangle = \frac{\alpha\eta G}{2\sqrt{2}m}\int[\rho_{532}(r) + \rho_{413}]\rho'(r)dV,$$
$$\rho_{532}(r) = \partial_z\langle 532|\sigma_z|532\rangle,$$
$$\rho_{413}(r) = \partial_z\langle 413|\sigma_z|413\rangle, \quad (32)$$

where ρ' is the octupole density given by Eq. (15). Note that the "spin densities" ρ_{532} and ρ_{413} depend on r, since the brackets $\langle..\rangle$ in the definitions of the densities in (32) denote averaging over spin only. Note also that the spin densities are T odd. Therefore, the BCS factor practically does not influence them. Numerical evaluation of integrals in Eq. (32) with Nilsson wave functions (A4) is straightforward, and the result is

$$\langle -|H_{TP}|+\rangle = \alpha\eta\beta_3\frac{G}{2\sqrt{2}m}\frac{3A}{4\pi R_0^4}[I_{413} + I_{532}]. \quad (33)$$

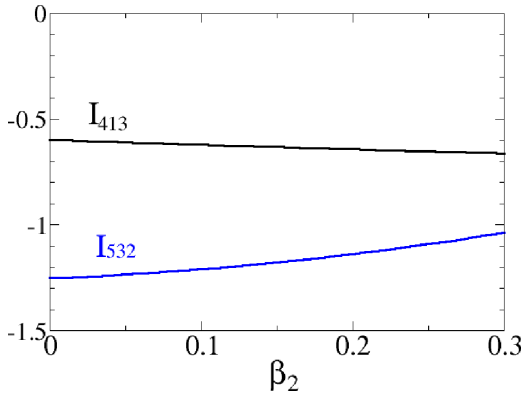

FIG. 4. Dimensionless matrix elements I_{413} and I_{532} vs quadrupole deformation.

The dimensionless quantities I_{413} and I_{532} are plotted in Fig. 4 versus β_2. At the physical deformation $\beta_2 = 0.29$, as in Eq. (11), their values are $I_{413} = -0.66$ and $I_{532} = -1.05$. Hence one arrives at the following value of the mixing matrix element:

$$\langle -|H_{TP}|+\rangle = -0.24\alpha\eta\beta_3 \text{ eV}. \tag{34}$$

The numerical coefficient in this equation depends on the explicit form of the Nilsson orbitals, given in Eq. (A4). The coefficients in the orbitals depend on the quadrupole deformation β_2, and, even though $\beta_2 = 0.29$ is known, there is an uncertainty in the coefficients related to a possible lack of accuracy of the Nilsson model. The plots of integrals I_{413} and I_{532} versus β_2, presented in Fig. 4, allow an estimate of the related uncertainty in Eq. (34). The integrals change with β_2 mainly due to the variation of the coefficients in the Nilsson orbitals' decomposition (A4). At $\beta_2 = 0$ the value of the relevant combination of integrals is $I_{413} + I_{532} = -1.85$ and at $\beta_2 = 0.3$ the same combination is -1.7. This variation is less than 10%. There may be other unaccounted components in the Nilsson orbitals. However, it is extremely unlikely that these small unaccounted components can change by more than 10% the value of the numerical coefficient 0.24 in Eq. (34).

IX. THE ELECTRIC DIPOLE MOMENT OF THE ^{153}Eu NUCLEUS

I need to determine the signs in Eqs. (3) and (4). In the accepted notation $\beta_3 > 0$ corresponds to the pear orientation with respect to the z axis shown in Fig. 5. According to Refs. [22–24] protons in an octupole-deformed nucleus are shifted in the positive z direction. Hence, d_z in Eq. (3) is positive, and, using Eqs. (6), one concludes that the sign in Eq. (4) is negative.

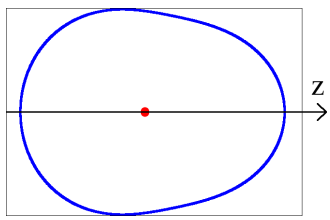

FIG. 5. The octupole pear shape with $\beta_2 = 0.29$ and $\beta_3 = 0.10$.

Using Eqs. (4) and (34), one finds the T- and P-odd electric dipole moment in the ground state:

$$\begin{aligned} d_z^{TP} &= 2\frac{\langle +|d_z|-\rangle\langle -|H_{TP}|+\rangle}{E_+ - E_-} \\ &= -0.59 \times 10^{-6}\alpha\beta_3\eta\,[e\,\text{fm}] \\ &= -1.18 \times 10^{-8}\eta\,[e\,\text{fm}]. \end{aligned} \tag{35}$$

For the numerical value I take $\alpha = 0.20$ [see Eq. (8)] and $\beta_3 = 0.10$ [see Eq. (29)]. Equation (35) gives the EDM in the corotating reference frame. The EDM of ^{153}Eu in the laboratory reference frame is

$$d^{TP} = \frac{5}{7}d_z^{TP} = -0.84 \times 10^{-8}\eta\,[e\,\text{fm}]. \tag{36}$$

This EDM is comparable with that of a heavy spherical nucleus (see Ref. [4]).

X. THE SCHIFF MOMENT OF THE ^{153}Eu NUCLEUS

The SM operator reads [4]

$$\hat{S}_z = \frac{1}{10}\left[\int \rho_q r^2 z dV - \frac{5}{3}r_q^2 d_z\right]. \tag{37}$$

It is a vector. Here ρ_q is the charge density and

$$r_q^2 \approx \tfrac{3}{5}R_0^2 \tag{38}$$

is the rms electric charge radius squared. With the static octupole deformation (15), the first term in Eq. (37) is given by

$$S_{\text{intr}} = \frac{1}{10}\int \rho_q r^2 z dV = \frac{9}{20\sqrt{35}\pi}eZR_0^3\beta_2\beta_3. \tag{39}$$

Here I use the same notation S_{intr} as that in Refs. [11,31]. The matrix element of the first term in (37) between the states (6) is

$$\langle +|\hat{S}_{1z}|-\rangle = -2\alpha S_{\text{intr}} = -\alpha\frac{9}{10\pi\sqrt{35}}eZR_0^3\beta_2\beta_3. \tag{40}$$

Combining this with Eq. (34), one finds the expectation value over the ground state:

$$\begin{aligned} \langle +|\hat{S}_{1z}|+\rangle &= 2\frac{\langle +|\hat{S}_{1z}|-\rangle\langle -|H_{TP}|+\rangle}{E_+ - E_-} \\ &= -0.24 \times 10^{-6}eZR_0^3\alpha^2\beta_2\beta_3^2\eta. \end{aligned} \tag{41}$$

Hence, the Schiff moment is

$$\begin{aligned} S_z &= \langle +|\hat{S}_z|+\rangle = \langle +|\hat{S}_{1z}|+\rangle - \frac{1}{10}R_0^2 d_z^{TP} \\ &= \left[-4.0 \times 10^{-3}\alpha^2\beta_2\beta_3^2 + 2.4 \times 10^{-6}\alpha\beta_3\right]\eta\,[e\,\text{fm}^3] \\ &= -4.16 \times 10^{-7}\eta\,[e\,\text{fm}^3]. \end{aligned} \tag{42}$$

For the final numerical value I take $\alpha = 0.20$ [see Eq. (8)], $\beta_2 = 0.29$ [see Eq. (11)], and $\beta_3 = 0.10$ [see Eq. (29)]. Note that the first term in the middle line of Eq. (42) is proportional to $\alpha^2\beta_3^2$ and the second term is proportional to $\alpha\beta_3$. This is

because one power of $\alpha\beta_3$ is "hidden" in the experimental dipole matrix element given by Eq. (4). The second term is about 10% of the first one. Equation (42) gives the Schiff moment in the corotating reference frame. The Schiff moment of ^{153}Eu in the laboratory reference frame is

$$S = \tfrac{5}{7}S_z = -2.97 \times 10^{-7}\eta\,[e\,\mathrm{fm}^3]. \tag{43}$$

This result is based on the single-particle T- and P-odd Hamiltonian (30). I believe that the theoretical uncertainty of the result is about a factor 2. This is mainly due to the uncertainty of the octupole deformation β_3, and can be further reduced by a more sophisticated analysis of inelastic electron scattering data [25], as pointed out in Sec. VII. However, the single-particle Hamiltonian (30) is obtained by mapping the two-nucleon T- and P-odd interaction to the effective single nucleon Hamiltonian. The two-nucleon T- and P-odd interaction itself originates from the quark level and also has some uncertainty. Reference [9] estimates the theoretical uncertainty of this mapping to be a factor 2. This estimate, based on the existing literature, is far from being certain and the problem requires further study. Let us note that the mapping from quark level to Eq. (30) is not nuclear specific. The mapping is irrelevant to the collective octupole deformation. Therefore, the mapping issue is separate from the collective octupole effect. The focus of the present paper is the calculation of the collective octupole contribution to the nuclear Schiff moment.

In the ^{151}Eu nucleus the energy splitting $E_- - E_+$ is 3.5 times larger than that in ^{153}Eu, and the quadrupole deformation is 2.5 times smaller. Therefore, the Schiff moment is at least an order of magnitude smaller than that of ^{153}Eu. Unfortunately, there are not enough available data to perform an accurate calculation for ^{151}Eu.

Another interesting deformed nucleus is ^{237}Np. Performing a simple rescaling from our result for ^{153}Eu one gets the following estimate of the ^{237}Np Schiff moment, $S \sim -1.5 \times 10^{-6}\eta\,[e\,\mathrm{fm}^3]$. This is 40 times larger than the single-particle estimate [4]. Following our method and using ^{238}U as a reference nucleus (like the pair ^{153}Eu and ^{152}Sm in the present paper), one can perform an accurate calculation of the ^{237}Np Schiff moment. Data for ^{238}U are available in Ref. [30].

XI. CONCLUSIONS

The Hamiltonian of nuclear time and parity violating interaction is given by Eq. (30). The connection between the dimensionless interaction constant η and the QCD axion θ parameter is discussed in Ref. [9]. The interaction (30) gives rise to the Schiff moment of a nucleus. In the present paper a method of calculating the Schiff moment of an even-odd deformed nucleus has been developed. This method is based on experimental data on magnetic moments and $E1$ and $E3$ transition amplitudes in the given even-odd nucleus and in adjacent even-even nuclei. Unfortunately such sets of data are not yet available for most of the interesting nuclei. Fortunately the full set of necessary data does exist for ^{153}Eu. Hence, using the new method, I perform the calculation for ^{153}Eu. The result is given by Eq. (43). The theoretical uncertainty of this result, about factor 2, is mainly due to the uncertainty in the value of the octupole deformation. A more sophisticated analysis of the available electron scattering data can further reduce this uncertainty.

The Schiff moment (43) is 20–50 times larger than that in heavy spherical nuclei [4] and it is three times larger than what Ref. [9] calls a "conservative estimate." On the other hand it is a factor of 30 smaller than the result of Ref. [11], based on the model of a static octupole deformation.

Using the calculated value of the Schiff moment, it is easy to rescale the results of Ref. [9] for the energy shift of the ^{153}Eu nuclear spin and for the effective electric field in the $EuCl_3 \cdot 6H_2O$ compound. The result of this rescaling is

$$\begin{aligned} \delta\mathcal{E}_o &= 0.9 \times 10^{-9}\theta\ [\mathrm{eV}], \\ E_o^* &= 0.3\,\mathrm{MV/cm}. \end{aligned} \tag{44}$$

These are the figures of merit for the proposed Cosmic Axion Spin Precession Experiment with $EuCl_3 \cdot 6H_2O$ [8].

ACKNOWLEDGMENTS

I am grateful to A. O. Sushkov for stimulating discussions and interest in the paper. This work has been supported by the Australian Research Council Centre of Excellence in Future Low-Energy Electronics Technology (Grant No. CE170100039).

APPENDIX: NILSSON WAVE FUNCTIONS

The parameters of the deformed oscillator potential used in the Nilsson model are as follows:

$$\begin{aligned} \omega_z &= \omega_0\left(1 - \frac{2}{3}\delta\right), \quad z_0 = \frac{1}{\sqrt{m\omega_z}}, \\ \omega_\rho &= \omega_0\left(1 + \frac{1}{3}\delta\right), \quad \rho_0 = \frac{1}{\sqrt{m\omega_\rho}}, \\ \omega_0 &= \frac{41\ \mathrm{MeV}}{A^{1/3}}, \end{aligned} \tag{A1}$$

where $m \approx 940$ MeV is the nucleon mass. The parameter δ is related to β_2 used in the main text:

$$\delta = \frac{3\sqrt{5}}{4\sqrt{\pi}}\beta_2 \approx 0.946\beta_2. \tag{A2}$$

The oscillator wave functions defined in Ref. [19] are

$$\begin{aligned} \overline{z} &= z/z_0, \\ |0\rangle_z &= \frac{1}{(\sqrt{\pi}z_0)^{1/2}}e^{-\overline{z}^2/2}, \\ |1\rangle_z &= \frac{\sqrt{2}}{(\sqrt{\pi}z_0)^{1/2}}\overline{z}e^{-\overline{z}^2/2}, \\ |2\rangle_z &= \frac{1}{(2\sqrt{\pi}z_0)^{1/2}}[2\overline{z}^2 - 1]e^{-\overline{z}^2/2}, \\ |3\rangle_z &= \frac{1}{(3\sqrt{\pi}z_0)^{1/2}}\overline{z}[2\overline{z}^2 - 3]e^{-\overline{z}^2/2}, \\ \overline{\rho} &= \rho/\rho_0, \end{aligned}$$

$$
\begin{aligned}
|2,2\rangle_\rho &= \frac{1}{\sqrt{2\pi}\,\rho_0}\overline{\rho}^2 e^{-\overline{\rho}^2/2}e^{2i\varphi},\\
|3,3\rangle_\rho &= \frac{1}{\sqrt{6\pi}\,\rho_0}\overline{\rho}^3 e^{-\overline{\rho}^2/2}e^{3i\varphi},\\
|4,2\rangle_\rho &= \frac{1}{\sqrt{6\pi}\,\rho_0}\overline{\rho}^2(\overline{\rho}^2-3)e^{-\overline{\rho}^2/2}e^{2i\varphi},\\
|5,3\rangle_\rho &= \frac{1}{\sqrt{24\pi}\,\rho_0}\overline{\rho}^3(\overline{\rho}^2-4)e^{-\overline{\rho}^2/2}e^{3i\varphi}.
\end{aligned}
\tag{A3}
$$

The Nilsson wave functions for the quadrupole deformation $\delta = 0.3$ written in the oscillator basis (A3) are [19]

$$
\begin{aligned}
\left|413\frac{5}{2}\right\rangle &= 0.938|1\rangle_z|3,3\rangle_\rho|\downarrow\rangle - 0.342|2\rangle_z|2,2\rangle_\rho|\uparrow\rangle\\
&\quad + 0.054|0\rangle_z|4,2\rangle_\rho|\uparrow\rangle,\\
\left|532\frac{5}{2}\right\rangle &= 0.861|3\rangle_z|2,2\rangle_\rho|\uparrow\rangle + 0.397|2\rangle_z|3,3\rangle_\rho|\downarrow\rangle\\
&\quad + 0.310|1\rangle_z|4,2\rangle_\rho|\uparrow\rangle + 0.075|0\rangle_z|5,3\rangle_\rho|\downarrow\rangle.
\end{aligned}
\tag{A4}
$$

[1] N. F. Ramsey, Annu. Rev. Nucl. Part. Sci. **32**, 211 (1982).
[2] A. P. Serebrov, E. A. Kolomenskiy, A. N. Pirozhkov, I. A. Krasnoshekova, A. V. Vasiliev, A. O. Polyushkin, M. S. Lasakov, A. N. Murashkin, V. A. Solovey, A. K. Fomin, I. V. Shoka, O. M. Zherebtsov, P. Geltenbort, S. N. Ivanov, O. Zimmer, E. B. Alexandrov, S. P. Dmitriev, and N. A. Dovator, Phys. Part. Nucl. Lett. **12**, 286 (2015).
[3] C. Abel *et al.*, Phys. Rev. Lett. **124**, 081803 (2020).
[4] O. P. Sushkov, V. V. Flambaum, and I. B. Khriplovich, Sov. Phys. JETP **60**, 873 (1984).
[5] L. I. Schiff, Phys. Rev. **132**, 2194 (1963).
[6] D. Budker, P. W. Graham, M. Ledbetter, S. Rajendran, and A. O. Sushkov, Phys. Rev. X **4**, 021030 (2014).
[7] T. N. Mukhamedjanov and O. P. Sushkov, Phys. Rev. A **72**, 034501 (2005).
[8] A. O. Sushkov, arXiv:2304.12105.
[9] A. O. Sushkov, O. P. Sushkov, and A. Yaresko, Phys. Rev. A **107**, 062823 (2023).
[10] N. Auerbach, V. V. Flambaum, and V. Spevak, Phys. Rev. Lett. **76**, 4316 (1996).
[11] V. V. Flambaum and H. Feldmeier, Phys. Rev. C **101**, 015502 (2020).
[12] J. Engel, J. L. Friar, and A. C. Hayes, Phys. Rev. C **61**, 035502 (2000).
[13] V. V. Flambaum and V. G. Zelevinsky, Phys. Rev. C **68**, 035502 (2003).
[14] R. B. Firestone, *Table of Isotopes*, 8th ed., edited by V. S. Shirley (Wiley-Interscience, 1996).
[15] V. B. Berestetskii, E. M. Lifshitz, and L. P. Pitaevskii, *Quantum Electrodynamics*, Course of Theoretical Physics Vol. 4, 2nd ed. (Butterworth-Heinemann, 1982).
[16] L. D. Landau and E. M. Lifshitz, *Quantum Mechanics: Non-Relativistic Theory*, Course of Theoretical Physics Vol. 3, 3rd ed. (Pergamon Press, Oxford, 1977).
[17] I. L. Lamm, Nucl. Phys. A **125**, 504 (1969).
[18] E. Tabar, E. Kemah, H. Yakut, and G. Hogor, Sakarya University Journal of Science **26**, 967 (2022).
[19] A. Bohr and B. R. Mottelson, *Nuclear Structure* (World Scientific, Singapore, 1998).
[20] O. P. Sushkov and V. B. Telitsin, Phys. Rev. C **48**, 1069 (1993).
[21] G. B. Hagemann, I. Hamamoto, and W. Satula, Phys. Rev. C **47**, 2008 (1993).
[22] G. A. Leander, W. Nazarewicz, G. F. Bertsch, and J. Dudek, Nucl. Phys. A **453**, 58 (1986).
[23] C. O. Dorso, W. D. Myers, and W. J. Swiatecki, Nucl. Phys. A **451**, 189 (1986).
[24] P. A. Butler and W. Nazarewicz, Nucl. Phys. A **533**, 249 (1991).
[25] W. Bertozzi, T. Cooper, N. Ensslin, J. Heisenberg, S. Kowalski, M. Mills, W. Turchinetz, C. Williamson, S. P. Fivozinsky, J. W. Lightbody, Jr., and S. Penner, Phys. Rev. Lett. **28**, 1711 (1972).
[26] G. A. Leander and R. K. Sheline, Nucl. Phys. A **413**, 375 (1984).
[27] Y. Cao, S. E. Agbemava, A. V. Afanasjev, W. Nazarewicz, and E. Olsen, Phys. Rev. C **102**, 024311 (2020).
[28] S. Ebata and T. Nakatsukasa, Phys. Scr. **92**, 064005 (2017).
[29] W. Zhang, Z. P. Li, S. Q. Zhang, and J. Meng, Phys. Rev. C **81**, 034302 (2010).
[30] A. Hirsch, C. Creswell, W. Bertozzi, J. Heisenberg, M. V. Hynes, S. Kowalski, H. Miska, B. Norum, F. N. Had, C. P. Sargent, T. Sasanuma, and W. Turchinetz, Phys. Rev. Lett. **40**, 632 (1978).
[31] V. Spevak, N. Auerbach, and V. V. Flambaum, Phys. Rev. C **56**, 1357 (1997).